International Journal of Pharmaceutics 417 (2011) 112–119

Contents lists available at ScienceDirect

International Journal of Pharmaceutics

journal homepage: www.elsevier.com/locate/ijpharm

Assessment of crystalline disorder in cryo-milled samples of indomethacin using atomic pair-wise distribution functions

Johan P. Bøtker[a,1], Pranav Karmwar[b,1], Clare J. Strachan[b], Claus Cornett[a], Fang Tian[c], Zoran Zujovic[c], Jukka Rantanen[a], Thomas Rades[b,*]

[a] Faculty of Pharmaceutical Sciences, Department of Pharmaceutics and Analytical Chemistry, University of Copenhagen, Universitetsparken 2, 2100 Copenhagen Ø, Denmark
[b] School of Pharmacy, University of Otago, 18 Frederick Street, Dunedin 9054, New Zealand
[c] Department of Chemistry, University of Auckland, Science Centre, Building 301, 23 Symonds St., Auckland, New Zealand

ARTICLE INFO

Article history:
Received 20 October 2010
Received in revised form
14 December 2010
Accepted 15 December 2010
Available online 21 December 2010

Keywords:
PDF
Indomethacin
Milling
DSC
XRPD
MVDA

ABSTRACT

The aim of this study was to investigate the usefulness of the atomic pair-wise distribution function (PDF) to detect the extension of disorder/amorphousness induced into a crystalline drug using a cryo-milling technique, and to determine the optimal milling times to achieve amorphisation. The PDF analysis was performed on samples of indomethacin obtained by cryogenic ball milling (cryo-milling) for different periods of time. X-ray powder diffraction (XRPD), differential scanning calorimetry (DSC), polarised light microscopy (PLM) and solid state nuclear magnetic resonances (ss-NMR) were also used to analyse the cryo-milled samples. The high similarity between the γ-indomethacin cryogenic ball milled samples and the crude γ-indomethacin indicated that milled samples retained residual order of the γ-form. The PDF analysis encompassed the capability of achieving a correlation with the physical properties determined from DSC, ss-NMR and stability experiments. Multivariate data analysis (MVDA) was used to visualize the differences in the PDF and XRPD data. The MVDA approach revealed that PDF is more efficient in assessing the introduced degree of disorder in γ-indomethacin after cryo-milling than MVDA of the corresponding XRPD diffractograms. The PDF analysis was able to determine the optimal cryo-milling time that facilitated the highest degree of disorder in the samples. Therefore, it is concluded that the PDF technique may be used as a complementary tool to other solid state methods and that further investigations are warranted to elucidate the capabilities of this technique.

1. Introduction

Many new chemical entities coming out of pharmaceutical drug discovery exhibit low aqueous solubility and subsequently poor bioavailability after oral administration (BCS class 2 drugs) (Patterson et al., 2005). It is therefore often required to enhance dissolution rate and solubility of these compounds, to allow further development of a drug into a medicine. One possible formulation route to achieve this is the conversion of a crystalline drug into an amorphous form. Several approaches can be taken to convert a crystalline form into its amorphous counterpart, including melting and quench-cooling, spray drying, and melt extrusion (Forster et al., 2001; Savolainen et al., 2007). These techniques have in common, that the crystalline form is immediately converted to a non-crystalline form (melt or solution), from which the amorphous solid is formed by cooling or precipitation. Another possible way to prepare amorphous forms is the direct conversion from a crystalline solid by mechanical activation (milling) (Chieng et al., 2006, 2008; Patterson et al., 2007).

However, the assessment of the resulting non-crystalline form in a milling operation is not without its challenges. It has previously been reported that different cryo-milling times and intensities yield compounds that have similar X-ray powder diffraction (XRPD) patterns, in which a broad halo was the only feature. This may be seen as an indication for amorphous conversion. However, differences in the differential scanning calorimetry (DSC) thermograms of these samples could be observed in form of increasing enthalpy of crystallisation (ΔH_C) and crystallisation temperatures (T_C) of the samples after extended cryo-milling times (Crowley and Zografi, 2002; Planinsek et al., 2010). This indicates that complete amorphisation may not have been achieved, despite the absence of peaks

Abbreviations: PDF, atomic pair-wise distribution function; XRPD, X-ray powder diffraction; DSC, differential scanning calorimetry; PLM, polarised light microscopy; ss-NMR, solid state nuclear magnetic resonances; MVDA, multivariate data analysis; NN, nearest neighbour; NNN, next nearest neighbour; NNNN, next nearest neighbour; LRO, long range order; SRO, short range order; ANOVA, analysis of variance; PCA, principal component analysis; SNV, standard normal variant transformation.

* Corresponding author. Tel.: +64 0 3 479 5410; fax: +64 0 3 479 7034.
E-mail addresses: thomas.rades@otago.ac.nz, thomas.rades@stonebow.otago.ac.nz (T. Rades).

[1] Both authors contributed equally to this work.

0378-5173/$ – see front matter © 2010 Elsevier B.V. All rights reserved.
doi:10.1016/j.ijpharm.2010.12.018

in the diffractograms, rendering XRPD an unsuitable method for determination of the optimal milling time for amorphisation of solids. However, atomic pair-wise distribution function (PDF) analysis of the corresponding XRPD diffractograms could be a possible route to gain a deeper insight into the degree of disorder in a milled sample. This is due to the fact, that the PDF displays the probability of finding two atoms separated with a given distance (Bates et al., 2006). Therefore, it could be expected that with increasing disorder in the sample, the signal amplitude of the PDF trace is further reduced, until the highest possible disorder for a given cryo-milling process has been achieved. If the PDF traces are monitored as a function of cryo-milling time, the optimal milling time for a mechanical activation process may be found.

The PDF technique utilizes a Fourier transformation of the XRPD diffractograms to produce a trace in a coordinate system. The Fourier transformation of the XRPD diffractograms is based on Eq. (1):

$$G(r) = \frac{2}{\pi}\int_0^{Q_{max}} Q[S(Q)-1]\sin(Qr)dQ \quad (1)$$

where $G(r)$ is a probability function and r is the distance separating the atoms. The structure function $S(Q)$, defined in Eq. (2), is the powder diffraction pattern that has been corrected for experimental errors and normalized and Q is the scattering vector as defined in Eq. (3).

$$S(Q) = \frac{I^{coh}(Q) - \sum c_i|f_i(Q)|^2}{\sum c_i|f_i(Q)|^2} + 1 \quad (2)$$

where $I^{coh}(Q)$ is the measured scattering intensity from a powder sample that has been properly corrected for background and other experimental effects and c_i and f_i are the atomic concentration and X-ray atomic form factor respectively.

$$Q = \frac{4\pi \sin\theta}{\lambda} \quad (3)$$

where θ is the angel between the incident and the diffracted beam and λ is the wavelength of the beam (Egami and Billinge, 2003).

The y-axis in the PDF trace is corresponding to the probability of finding two atoms separated by a distance stipulated by the x-axis. The PDF hence assesses the inter-atomic distances of the material. The PDF technique utilizes both the Bragg and diffuse scattering and is thus a total scattering technique. This is in contrast to conventional assessment of crystallinity where only the Bragg peaks are interpreted. In order to quantify the degree of disorder it is therefore advantageous to utilize the PDF technique since it also includes the diffuse scattering (Egami and Billinge, 2003).

The PDF technique has been used for several decades in the material science community (Billinge and Kanatzidis, 2004; Egami and Billinge, 2003; Proffen et al., 2003; Tarasov and Warren, 1936; Warren et al., 1936; Zernike and Prins, 1927) and has more recently been applied by the pharmaceutical community to study short and long range order of amorphous and glassy materials (Atassi et al., 2010; Bates et al., 2006; Heinz et al., 2008; Moore et al., 2009; Sheth et al., 2004, 2005). Some studies using PDF have investigated crystalline defects and helped in crystal structure determination (Atassi et al., 2010; Bates et al., 2007; Sheth et al., 2005). The PDF technique has also been used to characterise polymer/drug systems (Moore et al., 2009; Newman et al., 2008; Nollenberger et al., 2009) and the use of multivariate data analysis has alleviated the interpretation of the PDF (Heinz et al., 2008; Moore et al., 2009). There has been a widespread use of Cu X-ray sources for PDF analysis within the pharmaceutical area (Bates et al., 2006, 2007; Heinz et al., 2008; Moore et al., 2009; Newman et al., 2008; Nollenberger et al., 2009; Sheth et al., 2004, 2005). This is in contrast to the material science community which require synchrotron X-ray systems with small λ and hence large Q (Eq. (3)) to analyse inorganic compounds. However organic molecules have low atomic form factors which cause rapid X-ray intensity fall off. It is therefore possible to obtain PDFs from organic compounds using Cu X-ray sources with bigger λ and hence smaller Q (Bates et al., 2006).

Indomethacin has been utilized in several studies regarding amorphism and since its general properties are well described it was a good model compound for the experiments carried out in this work (Andronis et al., 1997; Andronis and Zografi, 2000; Crowley and Zografi, 2002; Patterson et al., 2005; Planinsek et al., 2010; Savolainen et al., 2007; Yoshioka et al., 1994).

The aim of this study was to investigate the usefulness of PDF to detect the extension of disorder/amorphousness induced into a crystalline drug using a cryo-milling technique, and to determine the optimal milling times to achieve amorphisation.

2. Materials and methods

2.1. Materials

Indomethacin (98%), (γ-form) was purchased from Chemie Brunschwig AG (Basel, Switzerland). Ethanol (analytical grade) was obtained from Merck (Darmstadt, Germany).

2.2. Preparation of polymorphs

The γ-form of indomethacin was used as received. The α-form of indomethacin was obtained by dissolving the γ-form in ethanol at 80 °C and then adding distilled water (at room temperature) to initiate precipitation. The precipitated crystals were removed by filtration and then dried under vacuum at room temperature (Savolainen et al., 2007).

2.3. Preparation of cryo-milled indomethacin samples

Amorphous indomethacin was prepared from both the α- and γ-forms of the drug. The crystalline starting materials were milled using an oscillatory ball mill (Mixer Mill MM301, Retsch GmbH & Co., Haan, Germany). The sample powder (1.0 g) was placed in a 25 mL volume stainless steel milling jar containing eight 9 mm diameter stainless steel balls. The jars were immersed in liquid nitrogen for three min after adding the sample, and then milled at 30 Hz. Milling was performed from 15 min to 420 min and the jars were recooled in liquid nitrogen for 3 min after every 15 min of milling. The 0, 15, 30, 45, 60, 90 and 120 min time point samples were measured in triplicate and the 195, 345 and 420 min time point samples in duplicate.

2.4. Sample storage

The freshly prepared amorphous samples were stored in a −80 °C freezer immediately after preparation.

2.5. Differential scanning calorimetry (DSC)

DSC thermograms were recorded on a DSC Q100 calorimeter (V8.2 Build 268, TA Instruments, New Castle, USA) after calibration for temperature and enthalpy using indium. Samples (2–5 mg) were crimped in an aluminium pan and heated at a rate of 10 K min^{-1} from 0 to 180 °C under a nitrogen gas flow of 50 mL min^{-1}. The glass transition temperature (T_g), crystallisation temperature (T_c) and melting temperature (T_m) were determined using TA Universal Analysis software (version 4.0C). The T_g was defined as the midpoint of the change in heat capacity of the sample, while both T_c and T_m were defined using the onset temperatures. Analysis of variance (ANOVA) was performed on the thermal events

Table 1
Thermal properties of γ-indomethacin and cryo-milled samples of γ-indomethacin milled for different times.

Cryo-milling time	T_g (°C)	±S.D.	Onset of crys. (°C)	±S.D.	Enthalpy of crys. (J/g)	± S.D.	Melting point (°C)	±S.D
0 min	–	–	–	–	–	–	159.9	0.20
15 min	34.5	2.83	52.5	1.64	32.6	0.85	158.2	0.07
30 min	32.9	1.23	56.7	1.67	35.9	3.75	158.3	0.32
45 min	34.6	0.09	58.6	0.97	37.9	1.47	158.2	0.25
60 min	32.9	2.07	64.0	0.90	36.8	1.34	158.2	0.35
90 min	36.0	1.92	76.2	2.2	37.5	3.46	157.2	0.37
120 min	33.3	2.71	77.6	2.83	42.8	3.71	157.5	0.28
195 min	30.4	0.16	83.2	7.93	61.2	18.36	158.7	0.13
345 min	32.6	0.30	85.9	7.27	75.3	3.29	157.1	1.42
420 min	31.7	5.00	88.7	10.83	65.1	5.93	158.1	0.25

using Microsoft Excel software (Microsoft Corporation, Washington, USA).

2.6. X-ray powder diffraction (XRPD)

Samples were analysed with a PANalytical X'Pert PROMPD system (PW3040/60, Philips, The Netherlands) using Cu Kα radiation with λ = 1.542 Å and a divergence slit of 1°. The samples were gently consolidated in a flat aluminium sample holder and scanned at 40 kV and 30 mA from 5° to 35° 2θ using a scanning speed of 0.1285 min^{-1} and a step size of 0.0084°. The diffraction patterns were generated using X'Pert High Score version 2.2.0 (Philips, The Netherlands). The experimentally obtained diffraction patterns were compared to the theoretical diffractograms, based on the crystal structures from the Cambridge Crystallographic Data Centre (CCDC). The data from the ref. codes INDMET02 and INDMET were used to generate the theoretical diffraction patterns of α- and γ-indomethacin, respectively (Cox and Manson, 2003).

2.7. Pair-wise distribution function (PDF)

Atomic pair-wise distribution function (PDF) analysis was performed by Fourier transforming the XRPD diffractograms using the freeware program RAD developed by V. Petkov at the University of Sofia, Department of Solid State Physics, Sofia-1126, Bulgaria. The setup for the program is described elsewhere (Petkov, 1989). The program can be downloaded at this site: http://www.pa.msu.edu/~petkov/software.html (accessed 1st of October 2010).

2.8. Multivariate data analysis (MVDA)

Principal components analysis (PCA) was used to help interpret differences in the diffractograms and PDF of the differently prepared amorphous forms. Before PCA, standard normal variant (SNV) transformation was performed to remove intensity differences unrelated to the sample composition and the spectra were then mean centered. The PDF data from 0 to 15 Å was omitted in order to exclude the influence from the short range order that can be observed in this region. PCA, preprocessing and scaling were performed using SIMCA P+ versions 12.0 (Umetrics AB, Umeå, Sweden).

2.9. Solid state nuclear magnetic resonance (ssNMR) spectroscopy

All ssNMR experiments were carried out using a Bruker AVANCE 300 spectrometer operating at 300.13 MHz proton frequency. Standard spectra were obtained by using the CP MAS (Cross-Polarization Magic Angle Spinning) technique. The experiments were carried out using a 7 mm Bruker spinning probe with zirconia rotors. The magic angle was adjusted by maximizing the sidebands of the ^{79}Br signal of a KBr sample. The proton 90° pulse duration was 4.2 μs and the field strength of the continuous wave decoupling field was 62.5 kHz. The contact time was 1.5 ms. The spectral width was 40 kHz. The ^{13}C chemical shift scale is referenced to TMS. The samples were rotated at 7000 ± 1 Hz.

3. Results and discussion

3.1. DSC

The DSC thermograms (Table 1) showed that all cryo-milled samples exhibited a T_g and a re-crystallization which was not observed for the crude α- and γ-indomethacin. Furthermore, the crude γ-indomethacin and the cryo-milled samples exhibited an endothermic melting event at 159 °C and the crude α-indomethacin at 154 °C. The presence of a T_g indicates that 15 min of cryo-milling with the aforementioned settings was sufficient to obtain amorphous indomethacin. The cryo-milled samples did not display any significant differences in the T_g position ($P > 0.2$). In contrast, the onset of crystallisation temperature increased significantly as a function of cryo-milling time with a correlation coefficient of 0.927 for the time points up to 120 min (Fig. 1). Similar observations have previously been reported for both the increase in enthalpy of crystallisation and the increase in re-crystallisation temperature after extended cryo-milling times (Crowley and Zografi, 2002; Planinsek et al., 2010). This correlation was believed to be caused by reduction in the number of nuclei as a function of cryo-milling time (Planinsek et al., 2010). Cryo-milling times of more than 120 min were however seen to have a smaller effect on the onset of crystallisation (Fig. 1).

The enthalpy of crystallisation also exhibited a positive correlation with the cryo-milling time (a correlation coefficient of 0.782 was obtained for the time points up to 420 min of cryo-milling). Although this relationship is not robust (no significant difference

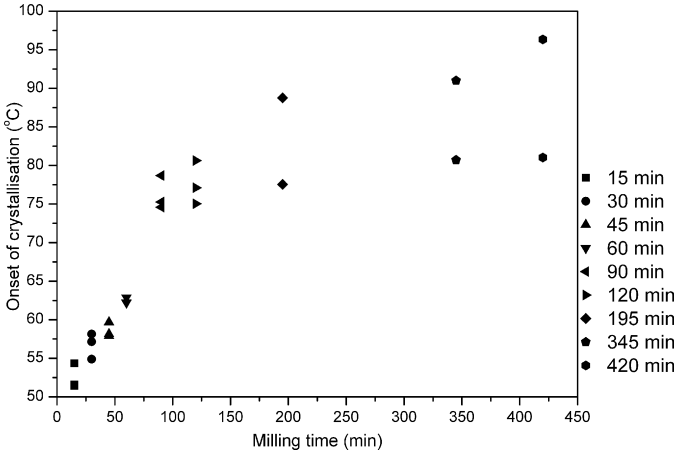

Fig. 1. Onset of crystallization as a function of milling time for the cryo-milled samples of γ-indomethacin (time in the figure correspond to the milling times).

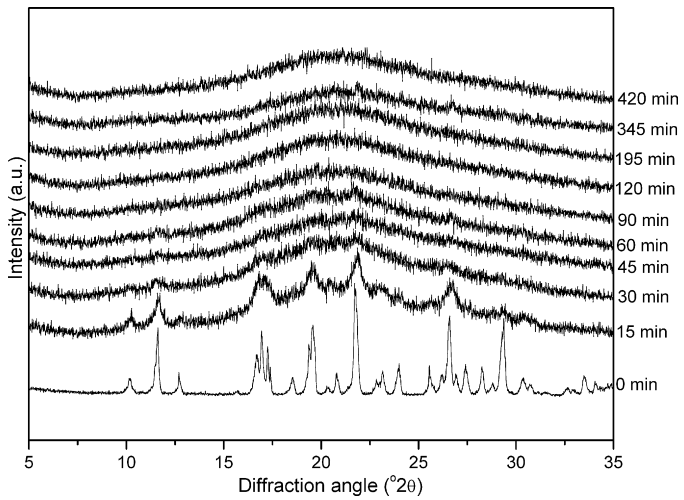

Fig. 2. XRPD diffractograms of the cryo-milled samples of γ-indomethacin milled for different times (time in the figure correspond to the milling times).

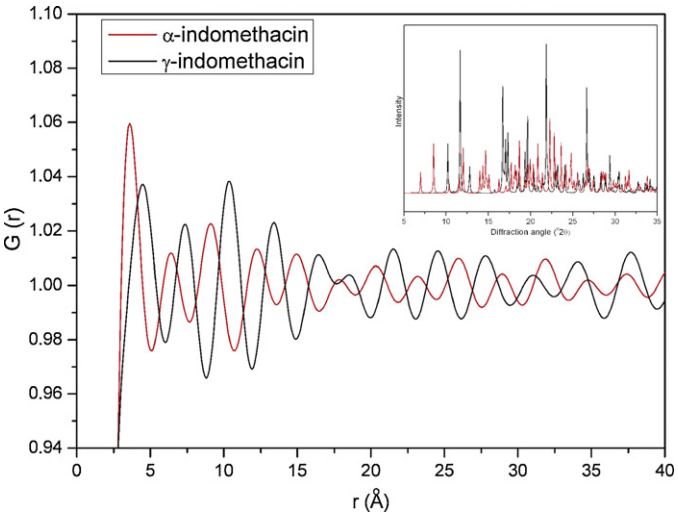

Fig. 3. PDF of the γ-form and α-form of indomethacin. XRPD diffractograms of γ-form and α-form of indomethacin are shown in the inset.

could be found between the 15, 30, 45, 60 and 90 min cryo-milled samples, $p > 0.1$), it nevertheless indicates that a reduction of the number of nuclei may not be the only process occurring in the samples upon increasing the milling time, but that the degree of disorder in the solid may in fact increase as a function of milling time and contribute to increasing crystallisation enthalpies.

It can therefore be proposed that cryo-milling for up to 120 min induces increasing disorder in the samples since an increase in the onset of crystallisation as a function of cryo-milling time was observed for this time interval. However, this increase in the onset of crystallisation as a function of cryo-milling time is absent when cryo-milling is performed for more than 120 min. This indicates that no or only little further disorder is obtained for the samples when cryo-milling is carried out for more than 120 min.

3.2. XRPD

The characteristic peaks of the γ-form were present in the samples cryo-milled for 15 min and are likely to stem from residual crystallinity, since all of the 15 min cryo-milled samples possessed a T_g. Samples cryo-milled for 30 min or more displayed no visible difference in their diffractograms. Complete lack of diffraction peaks in the diffractograms for the 30 min or longer cryo-milled samples revealed that indomethacin was completely "X-ray amorphous" regardless of milling time (Fig. 2). This indicates that XRPD was only capable of displaying visual differences in the degree of disorder until 30 min of cryo-milling. In contrast, in the DSC data differences in the onset of crystallisation until 120 min of cryo-milling were found.

3.3. PDF

The PDF of the two polymorphs of indomethacin (Fig. 3) showed a clear difference between the α- and γ-form. This difference was seen throughout the monitored region 0–40 Å. The PDF displayed in Fig. 4 represents the various cryo-milled samples as well as the crystalline γ-indomethacin. The value of the *y*-axis in the PDF trace is corresponding to the probability of finding two atoms separated with the distance stipulated by the *x*-axis. The peaks in the PDF trace are therefore representing the commonly occurring inter-atomic distances in the material. It is observed that the signal amplitude of the PDF trace of all the samples attenuates at varying rates towards unity at distances of large spatial separation. These concurrencies are in accordance with the fact that the finite *Q* resolution (Eq. (3)) will make a crystalline PDF trace attenuate and samples that are disordered will thus exhibit an even faster PDF trace attenuation. Consequently, this attenuation rate can be used to assess the degree of disorder in the samples (Dinnebier and Billinge, 2008).

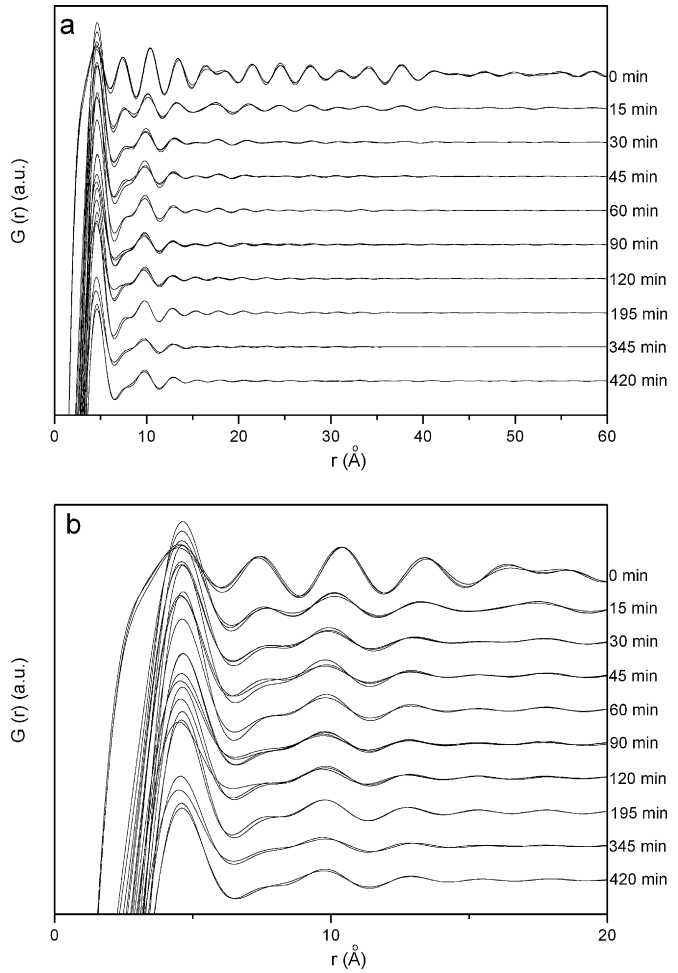

Fig. 4. PDF of cryo-milled samples of γ-indomethacin and γ-indomethacin. 0–60 Å (a); 0–20 Å (b).

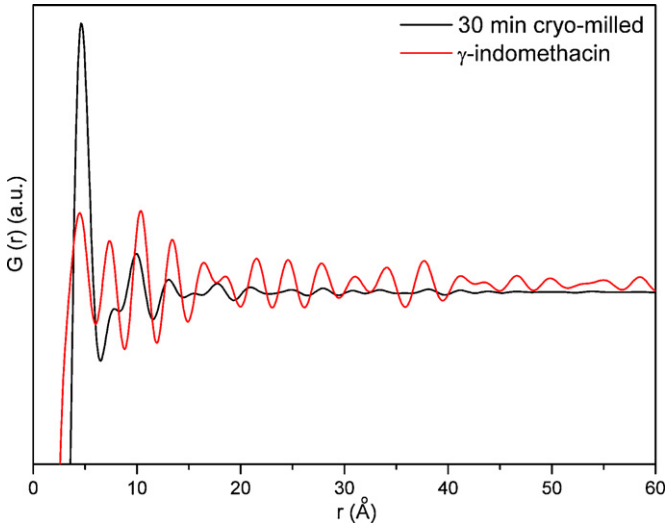

Fig. 5. PDF of γ-indomethacin and a 30 min cryo-milled sample of γ-indomethacin.

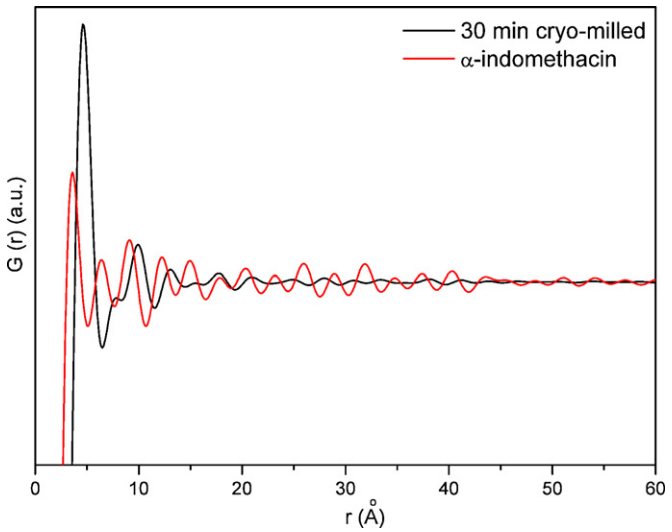

Fig. 6. PDF of α-indomethacin and a 30 min cryo-milled sample of γ-indomethacin.

3.3.1. Short range order (SRO)

In the PDF trace it was observed that some of the peaks below 15 Å are less affected by extended cryo-milling times (Fig. 4(a)). This conservation of peak intensity in the short range order (SRO) was stemming from the nearest neighbour (NN), next nearest neighbour (NNN) and next nearest neighbour (NNNN) interactions between molecules that are expected to be present in most amorphous systems (Bates et al., 2006; Fontana et al., 2004). Furthermore, it can be seen that the PDF traces of the cryo-milled samples had a high similarity to the PDF trace of the crude γ-indomethacin samples.

The first peak in the PDF data was located at 4.6–4.7 Å for all of the samples (Fig. 4(b)). This NN peak corresponds to the molecular thickness of indomethacin when the van der Waals radii were included (Bates et al., 2006). The second peak (NNN) was experiencing a peak shift between the crystalline material (located at 7.4 Å) and the rest of the samples (located at 7.8 Å). The width of the indomethacin molecule is approximately 7.3 Å so it might be inferred that this intermolecular distance reflects this width (Bates et al., 2006). The third peak (NNNN) is located at 10.4 Å for the crystalline material and at 9.8 Å for the rest of the samples. These distances might reflect the average cell length of the γ-indomethacin dimers which is approximately 10.0 Å. The peak shifts from the crystalline to the milled samples are indicating a collapse of the structure (Atassi et al., 2010). This collapse can be seen especially in the NNN peak intensity that becomes less pronounced as a function of extended cryo-milled time.

3.3.2. Long range order (LRO)

It can be seen from Fig. 4 that even though the cryo-milled samples retained most of the peak intensity for the NN and NNNN atoms there was a substantial intensity lowering of the peaks corresponding to atoms separated by greater distances. This reduction in peak intensity for the long range order appears to be correlated to the cryo-milling time. Thus PDF indicates that cryo-milling resulted in loss of (residual) long range order in the milled samples as a function of milling time and is a measure of the impaired crystallinity in the milled samples (Bates et al., 2006; Sheth et al., 2005)

Even though there were observable peak shifts and peak intensity losses in the cryo-milled samples the overall peak pattern of the cryo-milled samples was highly similar to the crystalline γ-indomethacin. This can be seen by overlaying the PDF of a 30 min γ-indomethacin cryo-milled sample over crystalline γ-indomethacin (Fig. 5) and crystalline α-indomethacin (Fig. 6). From comparison of Figs. 5 and 6 it is apparent that the similarities between the cryo-milled samples and the crystalline γ-indomethacin are higher than any similarity between the milled samples and the crystalline α-indomethacin. This indicates that the cryo-milled samples of γ-indomethacin retain some residual order of the γ-indomethacin (Bates et al., 2006) and is a testimony of preserved distances of the same atomic pairs (Atassi et al., 2010; Billinge et al., 2010). It has previously been reported that grinding of γ-indomethacin at approximately 4 °C leads to the formation of the γ-form upon re-crystallisation (Otsuka and Kaneniwa, 1988) so these data are in good agreement with the literature.

3.4. MVDA

MVDA was carried out on the PDF data to assess the structural disorder induced by cryo-milling. The PCA plot (Fig. 7) utilized two components to explain 96.9% of the variation and achieved a predictability of 95.5%. It can be seen that the crystalline γ-indomethacin samples were separated in the score plot from the 15 to 420 min cryo-milled samples (defined by the 1st principal component. Note that PC1 describes 91.5% of the variance of the dataset while PC2 describes 5.5%. This means that the separation along PC2 in the scores plot is visually exaggerated). Furthermore it is observed that the remaining milled samples appears along a trajectory (mainly defined by the 2nd principal component) starting with the 15 min cryo-milled sample and then proceeds

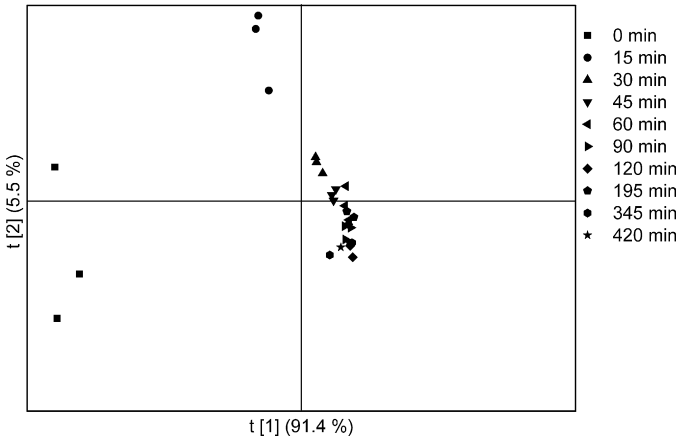

Fig. 7. Scores plot of the PDF data of cryo-milled samples of γ-indomethacin milled for different times.

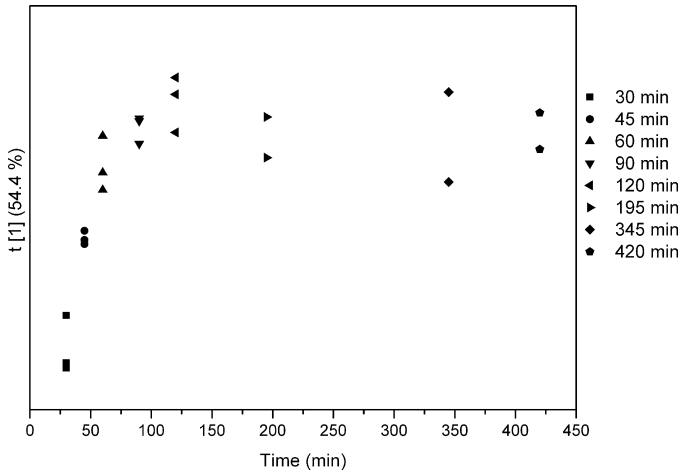

Fig. 8. Scores plot of the centered PDF data using one principal component excluding the crystalline γ-indomethacin and the 15 min cryo-milled samples of γ-indomethacin.

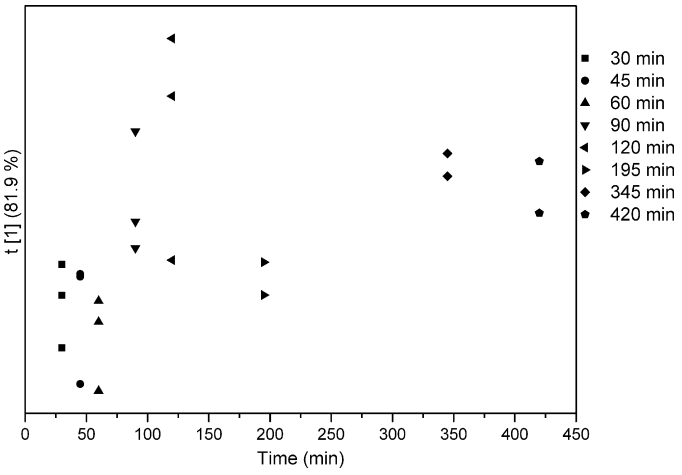

Fig. 10. Scores plot of centered XRPD diffractograms excluding the γ-indomethacin and the 15 min cryo-milled samples of γ-indomethacin.

consistently according to increasing cryo-milling times. However, it was also observed that the incremental differences between the samples get increasingly smaller for the extended cryo-milling times and after 120 min of cryo-milling time no further effect from cryo-milling is observed.

As mentioned above, the XRPD diffractograms were broad and featureless when cryo-milling was performed for 30 min or more. The PCA score plot in Fig. 8 displays the PDF data excluding γ-indomethacin and 15 min cryo-milled samples using only one principal component to explain 54.4% of the variation in the data and a predictive variable of 50.8%. Even though both, the explanation of variation and the predicting variable are quite low (only one principal component was used to facilitate visualisation) good agreement between the PDF data (Fig. 8) and the onset of crystallisation data (Fig. 1) was found. Both the PDF and DSC data indicate that there is a substantial effect from cryo-milling on the samples for up to 120 min of milling time. Furthermore, both the PDF and DSC data indicate that when cryo-milling was performed for 120 min or more no or only little further disorder is observed for the samples.

The PCA loading plot reveals that the principal component utilizes the peak intensity of the PDF to build the model (Fig. 9).

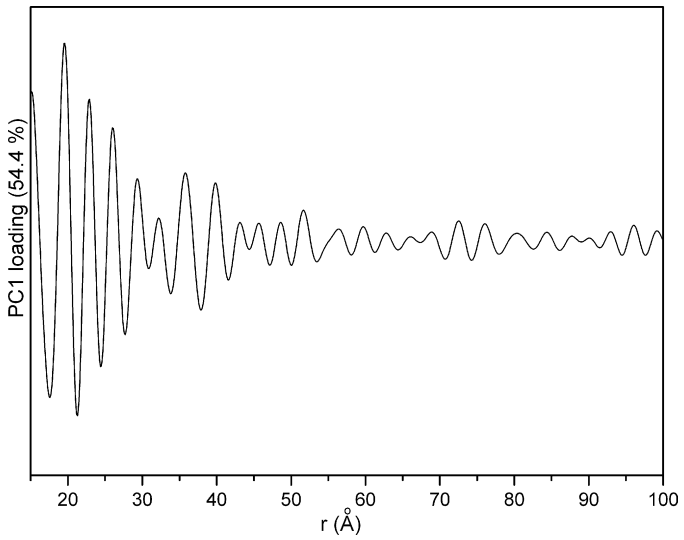

Fig. 9. Loadings plot of the PDF data using one component excluding the γ-indomethacin and the 15 min cryo-milled samples of γ-indomethacin.

Therefore, a reduction in peak intensity, and hence residual long range order, is detected.

In order to compare the PDF data to the original XRPD data, a PCA score plot of the XRPD data was devised that used only one principal component. The principal component explained 81.9% of the variation in the XRPD data and achieved a predictive power of 79.7% (Fig. 10). This PCA score plot however has limited use since the points are more or less randomly scattered throughout the plot. The PCA loading plot of the XRPD data shows that the model was built on the halo (data not shown). It was attempted to optimize the PCA model of the XRPD data by using SNV correction as a pre-processing tool. However, this approach was not successful since the PCA score plot of the SNV corrected XRPD data was only capable of explaining 19.2% of the variation in the XRPD data and achieved a predictive power of −0.06%. Furthermore, the PCA was incapable of differentiating between any of the time points (data not shown). Thus it can be concluded that the PDF data are superior to the original XRPD data in explaining the differences in the samples obtained by cryo-milling of γ-indomethacin for extended periods of time.

3.5. NMR

Solid state nuclear magnetic resonance (ss-NMR) was utilized to further explain the influence of cryo-milling on indomethacin. The NMR spectra indicate that there was a substantial effect from cryo-milling for different periods of time (Fig. 11(a)). This effect was seen in the changes of the spectral peaks at 90, 113, 116, 127, 134, 136, 143 and 168 ppm. However, the difference between the 60 and 90 min cryo-milled samples appears quite small, and were thus not further analysed. Furthermore, it was seen that the 60, 90 and 120 min cryo-milled samples do share a great resemblance with the spectrum of the crystalline γ-indomethacin.

There was no further evolution in the NMR spectra when cryo-milling was performed for more than 195 min (Fig. 11(b)) since the 195, 345 and 420 sample display the same ss-NMR spectra. Therefore, it can be concluded that the NMR data support the PDF and DSC data. NMR data also indicated that cryo-milling performed for more than 195 min had no additional effect on the samples.

3.6. Stability

The stability data indicate that there is a noticeable effect of cryo-milling time on the physical stability of the samples (time to onset of crystallisation, Fig. 12) for up to 120 min of milling.

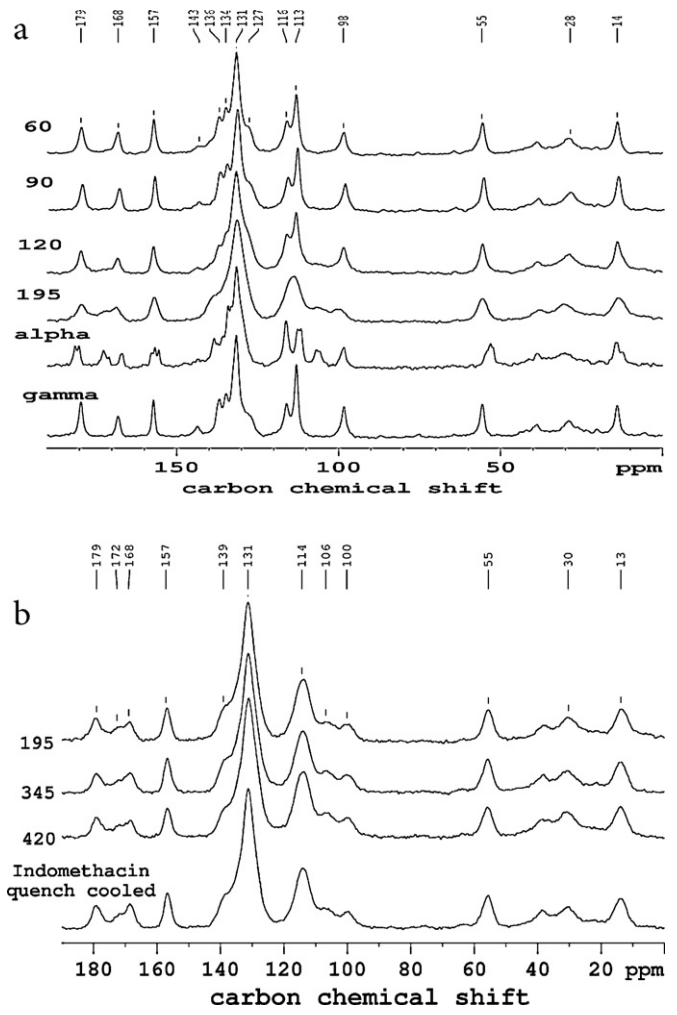

Fig. 11. NMR spectra of 60, 90, 120, 195 min cryo-milled samples of γ-indomethacin, and the α- and γ-indomethacin (a); NMR spectra of 195, 345 and 420 min cryo-milled samples of γ-indomethacin and quench cooled amorphous indomethacin (b).

When cryo-milling is performed for more than 120 min no further improvement in physical stability was found.

It has previously been observed that co-grinding of indomethacin with SiO_2 exhibited re-crystallisation kinetics which was affected by the milling time. It was shown that the re-crystallisation of the 180 min grinded samples was slower than the re-crystallisation of the 30 min grinded samples so our results are in good agreement with the literature (Watanabe et al., 2001). The stability data support the PDF, NMR and DSC data since they indicate that cryo-milling performed for 120 min or more has no additional effect on the samples.

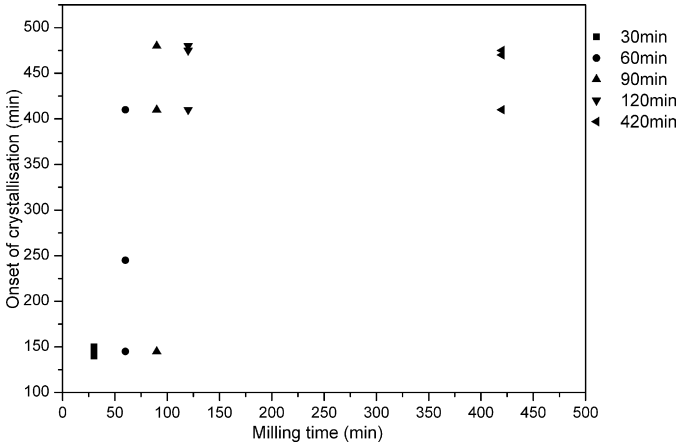

Fig. 12. Onset of crystallisation for 30, 60, 90, 120 and 420 min cryo-milled samples of γ-indomethacin (time in the figure correspond to the milling times).

4. Conclusion

This study explored the application of atomic pair-wise distribution functions (PDF) in assessing the disorder introduced in γ-indomethacin by cryogenic ball milling. Multivariate data analysis (MVDA) of the PDF is a much more efficient approach for differentiating the samples according to the degree of disorder, in comparison to the original XRPD diffractograms. The high similarity between the γ-indomethacin cryogenic ball milled samples and the crude γ-indomethacin indicated that milled samples retained residual order of the γ-form. The PDF technique encompassed the capability of achieving a correlation of the XRPD data with the physical properties determined from DSC, NMR and stability experiments. The PDF is therefore capable of assessing the minimal cryo-milling time that facilitates the highest degree of disorder and stability in the samples. PDF may be used as a complementary tool to other solid state techniques in the analysis of disorder in pharmaceutical solids.

References

Andronis, V., Yoshioka, M., Zografi, G., 1997. Effects of sorbed water on the crystallization of indomethacin from the amorphous state. J. Pharm. Sci. 86, 346–351.
Andronis, V., Zografi, G., 2000. Crystal nucleation and growth of indomethacin polymorphs from the amorphous state. J. Non-Cryst. Solids 271, 236–248.
Atassi, F., Mao, C., Masadeh, A.S., Byrn, S.R., 2010. Solid-state characterization of amorphous and mesomorphous calcium ketoprofen. J. Pharm. Sci. 99, 3684–3697.
Bates, S., Kelly, R.C., Ivanisevic, I., Schields, P., Zografi, G., Newman, A.W., 2007. Assessment of defects and amorphous structure produced in raffinose pentahydrate upon dehydration. J. Pharm. Sci. 96, 1418–1433.
Bates, S., Zografi, G., Engers, D., Morris, K., Crowley, K., Newman, A., 2006. Analysis of amorphous and nanocrystalline solids from their X-ray diffraction patterns. Pharm. Res. 23, 2333–2349.
Billinge, S.J., Kanatzidis, M.G., 2004. Beyond crystallography: the study of disorder, nanocrystallinity and crystallographically challenged materials with pair distribution functions. Chem. Commun. 7, 749–760.
Billinge, S.J.L., Dykhne, T., Juhas, P., Bozin, E., Taylor, R., Florence, A.J., Shankland, K., 2010. Characterisation of amorphous and nanocrystalline molecular materials by total scattering. CrystEngComm 12, 1366–1368.
Chieng, N., Rades, T., Saville, D., 2008. Formation and physical stability of the amorphous phase of ranitidine hydrochloride polymorphs prepared by cryo-milling. Eur. J. Pharm. Biopharm. 68, 771–780.
Chieng, N., Zujovic, Z., Bowmaker, G., Rades, T., Saville, D., 2006. Effect of milling conditions on the solid-state conversion of ranitidine hydrochloride form 1. Int. J. Pharm. 327, 36–44.
Cox, P.J., Manson, P.L., 2003. Indomethacin tert-butanol solvate at 120 K. Acta Crystallogr. Sect. E: Struct. Rep. Online 59, O1189–O1191.
Crowley, K.J., Zografi, G., 2002. Cryogenic grinding of indomethacin polymorphs and solvates: assessment of amorphous phase formation and amorphous phase physical stability. J. Pharm. Sci. 91, 492–507.
Dinnebier, R.E., Billinge, S.J.L., 2008. Powder Diffraction: Theory and Practice. Royal Society of Chemistry, Cambridge.
Egami, T., Billinge, S.J.L., 2003. Underneath the Bragg peaks: Structural Analysis of Complex Materials. Boston, Pergamon, Kiddington, Oxford, UK.
Fontana, M.P., Burioni, R., Cassi, D., 2004. The generalized Peierls–Landau instability: a novel perspective on the nature of glasses? Philos. Mag. 84, 1307–1311.
Forster, A., Hempenstall, J., Rades, T., 2001. Characterization of glass solutions of poorly water-soluble drugs produced by melt extrusion with hydrophilic amorphous polymers. J. Pharm. Pharmacol. 53, 303–315.
Heinz, A., Strachan, C.J., Atassi, F., Gordon, K.C., Rades, T., 2008. Characterizing an amorphous system exhibiting trace crystallinity. A case study with saquinavir. Cryst. Growth Des. 8, 119–127.
Moore, M.D., Steinbach, A.M., Buckner, I.S., Wildfong, P.L.D., 2009. A structural investigation into the compaction behavior of pharmaceutical composites using powder X-ray diffraction and total scattering analysis. Pharm. Res. 26, 2429–2437.
Newman, A., Engers, D., Bates, S., Ivanisevic, I., Kelly, R.C., Zografi, G., 2008. Characterization of amorphous API:polymer mixtures using X-ray powder diffraction. J. Pharm. Sci. 97, 4840–4856.

Nollenberger, K., Gryczke, A., Meier, C., Dressman, J., Schmidt, M., Brühne, S., 2009. Pair distribution function X-ray analysis explains dissolution characteristics of felodipine melt extrusion products. J. Pharm. Sci. 98, 1476–1486.

Otsuka, M., Kaneniwa, N., 1988. A kinetic-study of the crystallization process of noncrystalline indomethacin under isothermal conditions. Chem. Pharm. Bull. 36, 4026–4032.

Patterson, J.E., James, M.B., Forster, A.H., Lancaster, R.W., Butler, J.M., Rades, T., 2005. The influence of thermal and mechanical preparative techniques on the amorphous state of four poorly soluble compounds. J. Pharm. Sci. 94, 1998–2012.

Patterson, J.E., James, M.B., Forster, A.H., Lancaster, R.W., Butler, J.M., Rades, T., 2007. Preparation of glass solutions of three poorly water soluble drugs by spray drying, melt extrusion and ball milling. Int. J. Pharm. 336, 22–34.

Petkov, V., 1989. RAD, a program for analysis of X-ray diffraction data from amorphous materials for personal computers. J. Appl. Crystallogr. 22, 387–389.

Planinsek, O., Zadnik, J., Kunaver, M., Srcic, S., Godec, A., 2010. Structural evolution of indomethacin particles upon milling: time-resolved quantification and localization of disordered structure studied by IGC and DSC. J. Pharm. Sci. 99, 1968–1981.

Proffen, T., Billinge, S.J.L., Egami, T., Louca, D., 2003. Structural analysis of complex materials using the atomic pair distribution function – a practical guide. Z. Kristallogr. 218, 132–143.

Savolainen, M., Heinz, A., Strachan, C., Gordon, K.C., Yliruusi, J., Rades, T., Sandler, N., 2007. Screening for differences in the amorphous state of indomethacin using multivariate visualization. Eur. J. Pharm. Sci. 30, 113–123.

Sheth, A.R., Bates, S., Muller, F.X., Grant, D.J.W., 2004. Polymorphism in piroxicam. Cryst. Growth Des. 4, 1091–1098.

Sheth, A.R., Bates, S., Muller, F.X., Grant, D.J.W., 2005. Local structure in amorphous phases of piroxicam from powder X-ray diffractometry. Cryst. Growth Des. 5, 571–578.

Tarasov, L.P., Warren, B.E., 1936. X-ray diffraction study of liquid sodium. J. Chem. Phys. 4, 236–238.

Warren, B.E., Krutter, H., Morningstar, O., 1936. Fourier analysis of X-ray patterns of vitreous SiO_2 and B_2O_3. J. Am. Ceram. Soc. 19, 202–206.

Watanabe, T., Wakiyama, N., Usui, F., Ikeda, M., Isobe, T., Senna, M., 2001. Stability of amorphous indomethacin compounded with silica. Int. J. Pharm. 226, 81–91.

Yoshioka, M., Hancock, B.C., Zografi, G., 1994. Crystallization of indomethacin from the amorphous state below and above its glass-transition temperature. J. Pharm. Sci. 83, 1700–1705.

Zernike, F., Prins, J.A., 1927. Die beugung von röntgenstrahlen in flüssigkeiten als effekt der molekülanordnung. Z. Phys. A: Hadrons Nucl. 41, 184–194.